IOP Conf. Series: Journal of Physics: Conf. Series **869** (2017) 012024 doi:10.1088/1742-6596/869/1/012024

EPR studies for $GdBa_2Cu_3O_{7-\delta}$ added with nanosized ferrite $CoFe_2O_4$

H Basma[1], S Isber[2], S Noureldeen[3], M Anas[4] and R Awad[1]

[1]Physics Department, Faculty of Science, Beirut Arab University (BAU), Beirut.
[2]American University of Beirut, Department of Physics, Beirut, Lebanon.
[3]Physics Department, Faculty of Science, Lebanese University, Beirut.
[4]Physics Department, Faculty of Science, Alexandria University, Egypt.

Abstract. EPR measurements were conducted at different temperatures 100K ≤ T ≤ 295K for $GdBa_2Cu_3O_{7-\delta}$ superconducting samples prepared by the conventional solid state reaction technique, added with x wt.% nanosized ferrite of $CoFe_2O_4$,prepared by chemical co precipitation method, with 0 ≤x ≤ 0.40 wt.% . A broad isotropic symmetric EPR line with g factor g ≈ 2 is detected for the $(CoFe_2O_4)_xGdBa_2Cu_3O_{7-\delta}$ samples, corresponding to Gd^{3+} ions. The broadness is attributed to the superposition of signals resulting from the clustering of Gd^{3+} ions and the dipole interaction between these ions. The analysis of the absorption curve and its first derivative allowed to obtain several magnetic parameters including the number of spins N participating in EPR resonance which showed a decrease with increasing temperature and the activation energy E_a, which experienced a decrease with x.

1. Introduction

Electron paramagnetic resonance (EPR) serves as an effective tool to investigate the magnetic properties of high temperature superconductors. Awad *et al.* [1] conducted EPR studies of $GdBa_2Cu_{3-x}Ru_xO_{7-\delta}$. The results showed that the line symmetry is independent on both Ru-content and temperature while the magnetic parameters showed an increase with the Ru-content. Guskos *et al.* [2] measured the EPR spectra of $GdBaCu_3O_{7-\delta}$ (Gd-123) superconducting phase at different temperatures (4.2–120 K) and detected a signal from Gd^{3+} ions with g = 1.99 and a signal from Cu^{2+} ions with $g_x = 2.074$, $g_y = 2.015$ and g_z, = 2.202. Alekseevskii *et.al* [3-5] conducted EPR studies for $GdBa_2Cu_30_{7-\delta}$ with δ = 0.15 and 0.5. A single line spectrum of Gd^{3+} ions was observed for all samples. EPR measurements showed a metallic character for samples with δ =0.5, while resistivity measurements showed a semiconducting behavior. The EPR signal consisted of two signals with nearly equal g values (g -~ 1.99) but with two different line widths. For the first line, the line width linearly depends on the temperature. For the second one, the line width does not depend on the temperature and is equal to 1000 Oe. In this work, EPR measurements for $(CoFe_2O_4)_x$,Gd-123 with 0 ≤ x≤ 0.4 wt. % prepared by the conventional solid state reaction technique were conducted. The analysis of the absorption curve and its first derivative of the samples allowed the calculation of several magnetic parameters. The variations of these parameters are discussed with respect to the amount of nano ferrite addition and the variation of temperature.

2. Experimental techniques:

Nanosized $CoFe_2O_4$ powder and $(CoFe_2O_4)xGdBa_2Cu_3O_{7-\delta}$, $0.0 \le x \le 0.4$wt % samples were prepared by chemical Co-precipitation method and conventional solid-state reaction technique, respectively as reported

previously [6]. EPR measurements were performed using a Bruker microwave controller ER 048 spectrometer, operating at the X-band frequency (9.24 GHz). The magnetic field was scanned in the range 0–10000 G and a microwave power of 15mW. Powder sample of 100 mg was taken in a quartz tube for EPR measurements. The EPR spectra of the samples were recorded at temperature range (100–295K).

3. Results and Discussions:

The first derivative EPR absorption spectra at different temperatures (T=295, 263,233, 193, 163, 133 and 100K) for $GdBa_2Cu_3O_{7-\delta}$ are shown in figure 1. The EPR spectra contain a broad isotropic line corresponding mainly to Gd^{3+}ions [7] which is symmetric about its central position for all samples.

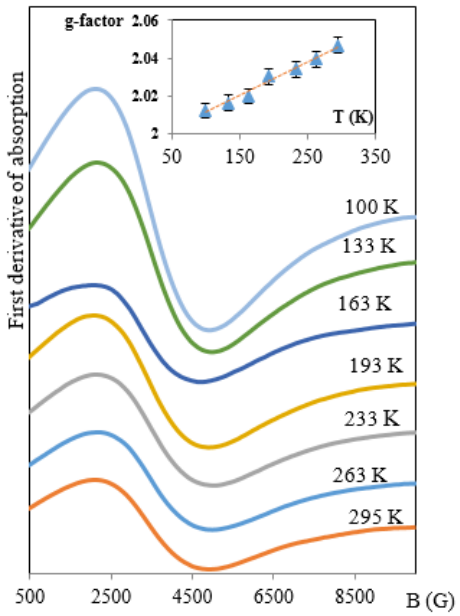

Figure.1: First-derivative absorption spectra for $GdBa_2Cu_3O_{7-\delta}$ versus the magnetic field at different temperatures. The inset represents the variation of g-factor versus temperature.

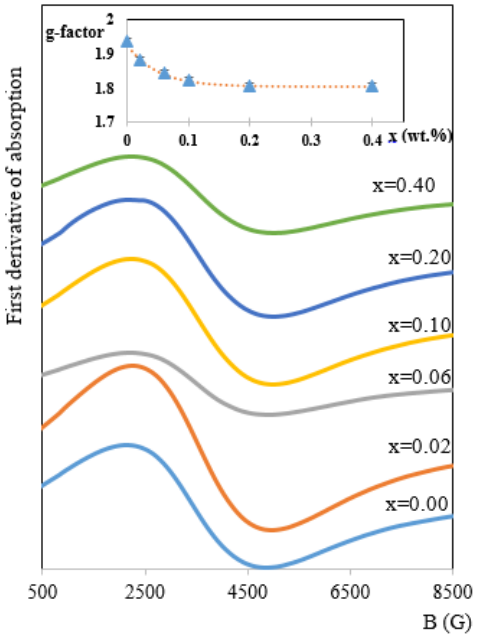

Figure.2: First-derivative absorption spectra versus magnetic field for $(CoFe_2O_4)_x$ $GdBa_2Cu_3O_{7-\delta}$phase at T = 100 K. The inset represents the variation of g-factor versus x.

The symmetric shape indicates the absence of skin effect [8]. The intensity of the EPR lines at liquid-nitrogen temperature is stronger than that at room temperature. The broadness of the EPR spectra for all samples can be attributed to one of three possible mechanisms. It may result from the dipole–dipole interactions between the Gd^{3+}ions or the modification of the degree of short-range ordering in the environment of the Gd^{3+} sites or the departure from a random spatial distribution of these sites in the glass network (clustering etc) [9].The values of the g-factor at different temperatures for $GdBa_2Cu_3O_{7-\delta}$ are shown in the inset of figure 1. A linear increase of the g- factor with temperature is observed for all samples. The slight temperature dependence of the g- factor, and its shift to lower values at lower temperatures can be related to the dynamic Jahn Teller (JT) effect [10,11]. Figure 2 shows the EPR Spectra for $(CoFe2O4)_xGdBa_2Cu_3O_{7-\delta}$ (x=0.01, 0.04, 0.06, 0.20 and 0.40 wt. %) samples at T =100 K. The inset of figure 2, shows the variation of the g- factor of $(CoFe2O4)_xGdBa_2Cu_3O_{7-\delta}$ for different values of x at T=100K. The values of the g-factor showed a decrease with x. This decrease can be attributed to the

environment changes around Gd^{3+} which contains Cu^{2+} magnetic ions and $BaCuO_2$ impurities detected from XRD measurements [12]. It is important to mention that the ferromagnetic resonance line FMR corresponding to Co^{2+} ions at $T \approx 100$ K, originated from Co moments in $CoFe_2O_4$ nanoferrites for $(CoFe_2O_4)_xGdBa_2Cu_3O_{7-\delta}$ doesn't not appear in the spectrum. The ferromagnetic order is caused by an antisymmetric exchange coupling between neighboring Co moments. The disappearance of FMR line confirms the electrical resistivity data which did not show a ferromagnetic order at $T = 100$ K [12].

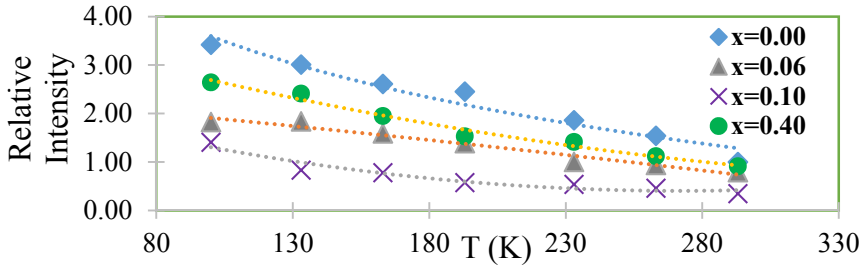

Figure 3: Temperature dependence of the EPR relative intensity for $(CoFe_2O_4)_x$.

The variation of The EPR relative intensity as a function of temperature is shown in Figure 3 for x=0.0, 0.06, 0.10 and 0.40.The EPR line intensity increases as the temperature decreases from room temperature to 100 K. The EPR line intensity is proportional to the magnetic susceptibility of the localized moments spin system. The magnetic susceptibility obeys Curie–Weiss law for a temperature higher than T_c for Gd-123 phase [13]. The EPR relative intensity decreases with the increase in x indicating that the addition of Co Fe_2O_4 nano ferrite suppressed the unpaired electrons in Gd-123 phase and consistent with the XRD results that showed a reduction in the Gd-123 phase and an enhancement in the $BaCuO_2$ impurity phase with the increase of x [12].

Figure 4 shows the temperature dependence of the peak-to-peak line width (ΔH_{pp}) for $(CoFe_2O_4)_xGdBa_2Cu_3O_{7-\delta}$. The line width shows a linear increase when the temperature increases from 100 to 295 K. The temperature dependence of the peak-to-peak line width can be fitted according to the relation:

$$\Delta H_{PP} = A_{PP} + B_{PP}T \quad (1)$$

Where A_{pp} is the residual line width and B_{pp} is the thermal broadening, corresponding to the Korringa-type interaction between the paramagnetic ions with the host conduction carriers through the exchange interactions J_s [14]. The values of A_{pp} and B_{pp} are listed in table 1. The values of B_{pp} show a decrease with the increase in x. The fitting parameter B_{pp} is proportional to the density of state which is proportional to the number of carriers [15]. A similar trend was observed for the variation of the hole carriers' concentration at CuO_2 planes with $CoFe_2O_4$ addition from previous RBS measurements [16].The number of spins (N) participating in the resonance was calculated by comparing the area under the absorption curve of the virgin samples at different temperatures with that of the standard $CuSO_4.5H_2O$ [15]. Figure 5 shows the logarithmic plot of N as a function of the reciprocal of absolute temperature. A linear relation between $\log(N)$ and $1/T$ is found as expected from Boltzmann law. The activation energy E_a was calculated from the slope of the lines and the values of E_a are also listed in table 1. The activation energy shows a similar trend to that of B_{pp} resulting from the suppression of N with the addition of $CoFe_2O_4$.

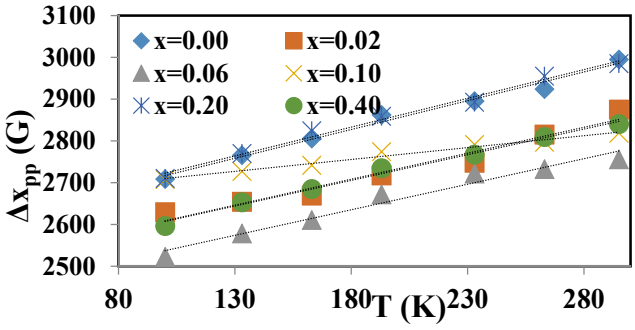

Figure 4: Variation of ΔH_{pp} with temperature.

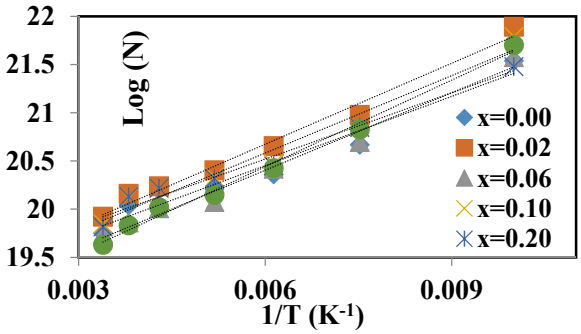

Figure 5: Log (N) as a function of (1/T).

Table1: The variation of A_{pp}, B_{pp} and E_a as a function of x.

x	0.00	0.02	0.06	0.10	0.20	0.40
Bapp (G/K)	1.378	1.242	1.225	1.568	1.178	1.128
App (G)	2579.2	2448.8	2415.2	2653.2	2585.2	2484.4
Ea (eV)	0.0258	0.0248	0.0231	0.023	0.0197	0.0208

4. Conclusion

The EPR studies of Gd-123 superconducting samples added with x wt. % of $CoFe2O_4$ nano ferrites were conducted. The line width showed an increase with temperature, the logarithmic plot of the number of spins with (1/T) showed a linear dependence. The magnetic parameters including the thermal broadening (B_{pp}), the number of spins (N) and the activation energy (E_a) were suppressed with the increase in x.

References

[1] Awad R *et al* 2012 *Physica* C*: Superconductivity*, **477** 74-83
[2] Guskos N *et al Phys.* 1990 *Stat. Sol. (b)* **162** 243
[3] Alekseevskii N E *et al* 1988 *JETP Lett*. **48** 37
[4] Alekseevskii N E *et al* 1989 *J. Low Temp. Phys.* **77** 87
[5] Garifullin I A 2015 *J. Low Temp. Phys.* **178** 243
[6] Awad R *et al* 2015 *Journal of Superconductivity and Novel Magnetism* **28(2)** 535-539
[7] Nakamura F *et al* 1989 *Physica* C*: Superconductivity*, **162** 1287-1288
[8] Bejjit L and Haddad M 2002 *Physica* C*: Superconductivity* **371(4)**, 339-343
[9] Kliava J *et al* 2003 *Journal of Physics: Condensed Matter* **15(40)** 6671
[10] O'Brien M C, In Proceedings of the Royal Society of London (Vol. **281**, No. 1386, pp. 323-339).
[11] Riley M *et al* 1986 *Chemical physics*, **102(1)** 11-28
[12] Awad R *et al* 2014 *Journal of Superconductivity and Novel Magnetism* **27** no 7 1757-1767.
[13] Kikuchi H *et al* 1988 *Journal of the Physical Society of Japan* **57(6)** 1887-1890
[14] Barnes S E 1981 *Advances in Physics*, **30(6)** 801-938
[15] Weil J A and Bolton J R John 2007 Wiley & Sons.
[16] Basma H *et al* 2015 *Materials Sciences and Applications*, ***6* (09)** 828